

## BACKGROUND GEOMETRY IN 4D CAUSAL DYNAMICAL TRIANGULATIONS\*

ANDRZEJ T. GÖRLICH

Institute of Physics, Jagellonian University  
Reymonta 4, 30-059 Kraków, Poland

*(Received October 21, 2008)*

The method of Causal Dynamical Triangulations is a background independent approach to Quantum Gravity. Imposing causal structure of the universe we observe a classical 4D de Sitter spacetime as a “background” geometry. From the study of the spatial volume fluctuations one can determine the effective action for the scale factor. In this approach one obtains a minisuperspace model which has a maximum symmetry by integrating out all degrees of freedom except the scale factor and not by freezing them.

PACS numbers: 98.80.Qc, 04.60.Gw, 04.60.Nc

### 1. Introduction

The basic tool used in the approach presented below is a path-integral formalism applied to quantize a theory of gravity. The partition function of quantum gravity is defined as a formal integral over all geometries,

$$Z = \int \frac{\mathcal{D}\mathcal{M}[g]}{\text{Diff}_{\mathcal{M}}} e^{iS^{\text{EH}}[g]}, \quad (1)$$

weighted by the Einstein–Hilbert action,

$$S^{\text{EH}}[g] = -\frac{1}{G} \int dt \int d\Omega \sqrt{-\det g} (R - 6\lambda), \quad (2)$$

where  $G$  and  $\lambda$  are, respectively, the gravitational and cosmological constants, and  $R$  denotes the scalar curvature. In this expression we should integrate over equivalence classes of metrics, *i.e.* divide out a volume of the diffeomorphism group  $\text{Diff}_{\mathcal{M}}$ .

---

\* Presented at the XLVIII Cracow School of Theoretical Physics, “Aspects of Duality”, Zakopane, Poland, June 13–22, 2008.

To make sense of the formal gravitational integral (1), the model of Causal Dynamical Triangulations uses a standard method of regularization, and replaces the path integral by a sum over a discrete set of all causal triangulations  $\mathcal{T}$ . Teitelboim [4, 5] pointed out the importance of causality in the quantum gravitational path integral, as a remnant of the Lorentzian signature. We assume the spacetime topology to be  $S^3 \times S^1$  and the existence of a global proper-time foliation, as an implication of causality. The spatial geometry at each discrete proper-time step is represented by a triangulation of  $S^3$ , made up of equilateral tetrahedra with a side length  $a_s > 0$ . Due to the global proper-time foliation, Wick rotation is well defined. As a consequence of the discretization procedure and rotation to the Euclidean signature, the partition function (1) is written as a sum

$$Z = \sum_{\mathcal{T}} \frac{1}{C_{\mathcal{T}}} e^{-S[\mathcal{T}]}, \quad (3)$$

where the factor  $1/C_{\mathcal{T}}$  is a symmetry factor, given by the order of the automorphism group of a triangulation  $\mathcal{T}$ . The explicit form of the discretized action  $S[\mathcal{T}]$  is evaluated in the next section.

It is impossible to evaluate partition functions (1) or (3) using purely analytical methods and we use Monte Carlo techniques to calculate the expectation values of observables. In this paper, the recent results obtained in the framework of Causal Dynamical Triangulations are presented. It is shown that the background geometry arises dynamically and that it has a form of a de Sitter space. Next, the effective action for quantum fluctuations is derived.

## 2. Fundamental building blocks of CDT

The building blocks of four dimensional Causal Dynamical Triangulations are four-simplices. Each simplex has five vertices, all of them connected to each other. The boundary of a simplex consists of five tetrahedral faces. A four-dimensional simplicial manifold, with a given topology, can be obtained by properly gluing pairwise simplices along common faces. The metric inside every simplex is flat.

The causal structure introduces a distinction between the time links of length  $a_t$  and the spatial links of length  $a_s$ . These lengths are assumed to be fixed for all simplices, opposite to the Regge's model [6]. Therefore, there are two kinds of four-simplices, first of a type  $\{4, 1\}$  with four vertices lying in one spatial slice and one in the neighboring slice, and second of a type  $\{3, 2\}$  with three vertices lying in one spatial slice and two in the adjacent slice. The two types of simplices differ in volume and angles. Each spatial slice is built from tetrahedra and has a  $S^3$  topology, which is not allowed to

change in time. The Wick rotation is well defined and it can be performed by the analytic continuation to imaginary lengths of the time links  $a_t \rightarrow ia_t$ .

Because no coordinates are introduced, the CDT model is manifestly diffeomorphism-invariant. Such a formulation involves only geometric invariants like lengths and angles. We define the geodesic distance of two simplices as the length of the shortest path on a lattice dual to the triangulation. A volume of the simplicial manifold is proportional to the number of simplices. Similarly, the curvature of a simplicial manifold can be expressed using the angle deficit which is localized at triangles.

### 2.1. Regge action

The action appearing in Eq. (3) is a discrete version of the Einstein–Hilbert action (2) and is called the Regge action. It is easy to see that, for any simplicial manifold  $\mathcal{T}$ , the total four-volume  $V_4 = \int dt \int d\Omega \sqrt{\det g}$  is a linear function of a total number of four-simplices  $N_4$  and a number of four-simplices of type  $\{4, 1\}$   $N_{41}$ . The proportionality coefficients are purely geometric and depend on  $a_t$  and  $a_s$  (see [1] for details). Similarly, it can be shown that the global curvature  $\int dt \int d\Omega \sqrt{\det g} R$  will depend on  $N_4$  and the total number of vertices  $N_0$ . The Regge action can be written in a very simple form,

$$S[\mathcal{T}] = -K_0 N_0[\mathcal{T}] + K_4 N_4[\mathcal{T}] + \Delta(N_{41}[\mathcal{T}] - 6N_0[\mathcal{T}]), \quad (4)$$

where  $K_0$ ,  $K_4$  and  $\Delta$  are bare coupling constants, and naively they are functions of  $G$ ,  $\lambda$  and  $a_t, a_s$ .  $K_4$  plays a similar role as a cosmological constant, it controls the total volume and needs to be kept near its critical value during numerical simulations.  $\Delta$  is related to the asymmetry factor between time and spatial link lengths. It is zero when  $a_t = a_s$  and does not occur in the Euclidean Dynamical Triangulations.  $\Delta$  will play an important role as it will allow to observe new phases.

## 3. Monte Carlo simulations

The idea which stands behind Monte Carlo simulations is to approximate the infinite sum which appears in the partition function (3) by a sum over a finite number of Monte Carlo configurations. More precisely, given an observable  $\mathcal{O}[g]$ , *e.g.* three-volume  $v(t)$  of a spatial slice at time  $t$ , we would like to calculate its expectation value  $\langle \mathcal{O}[g] \rangle$ . In the CDT framework the geometries  $[g]$  are already restricted to a discrete set of simplicial manifolds  $\mathcal{T}$  and

$$\langle \mathcal{O}[g] \rangle = \frac{1}{Z} \sum_{\mathcal{T}} \frac{1}{C_{\mathcal{T}}} \mathcal{O}[\mathcal{T}] e^{-S[\mathcal{T}]}, \quad (5)$$

where the partition function  $Z$  is given by Eq. (3) with the action (4).

The Monte Carlo simulations generate a finite set of configurations  $\{\mathcal{T}^{(1)}, \dots, \mathcal{T}^{(K)}\}$  and allow to approximate the average (5) by a summation over it,

$$\langle \mathcal{O}[g] \rangle \approx \frac{1}{K} \sum_{i=1}^K \mathcal{O}[\mathcal{T}^{(i)}]. \quad (6)$$

Let us notice, that no factor  $\frac{1}{C_{\mathcal{T}}} e^{-S[\mathcal{T}]}$  is needed, since configurations are generated according to the probability distribution  $P[\mathcal{T}] = \frac{1}{Z} \frac{1}{C_{\mathcal{T}}} e^{-S[\mathcal{T}]}$ , which means that more probable geometries will more likely appear in the set  $\{\mathcal{T}^{(1)}, \dots, \mathcal{T}^{(K)}\}$ . The larger is the number  $K$  of configurations and the smaller are the autocorrelations of  $\mathcal{T}^{(i)}$ , the more accurate is the approximation (6).

The Monte Carlo algorithm performs a random walk in the phase-space of configurations, *i.e.* space of piecewise linear geometries. The algorithm starts with a minimal configuration with a given topology  $S^3 \times S^1$ . Each step is one of the seven local moves of 4D CDT, so-called Alexander moves. The moves do not change the topology and do not spoil the global proper-time foliation. In order to probe the phase-space in agreement with the probability distribution  $P[\mathcal{T}]$ , several conditions must be fulfilled: The moves should be ergodic, which means that it is possible to reach every allowed configuration. The acceptance probability  $W(\mathcal{A} \rightarrow \mathcal{B})$  of a move from configuration  $\mathcal{A}$  to  $\mathcal{B}$  should satisfy the detailed balance condition:

$$P(\mathcal{A})W(\mathcal{A} \rightarrow \mathcal{B}) = P(\mathcal{B})W(\mathcal{B} \rightarrow \mathcal{A}).$$

After a sufficiently large number of steps, configurations are independent and can be added to the set  $\{\mathcal{T}^{(1)}, \dots, \mathcal{T}^{(K)}\}$ .

#### 4. Phase diagram

A value of the bare cosmological constant  $K_4$  is always tuned to its critical value, in order to keep the total volume fluctuating around a given finite value. The two remaining bare coupling constants  $K_0$  and  $\Delta$  can be freely adjusted and depending on their values we observe three qualitatively different behaviors of a typical configuration. An illustrative sketch of the phase diagram is presented in Fig. 1. For small values of  $\Delta$  and  $K_0$  all simplices are localized in one spatial slice and a dimension reduction is observed. This phase corresponds to so-called *crumpled phase* present in Euclidean Dynamical Triangulations [3]. For large values of  $K_0$  the universe disintegrates into uncorrelated irregular sequences of maxima and minima with time extension of few steps. This phase is related to so-called *branched polymers phase* also known from the Euclidean Dynamical Triangulations.

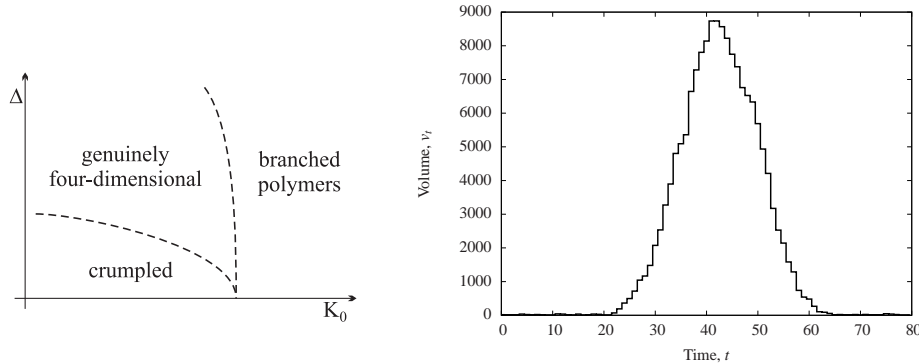


Fig. 1. Left: a qualitative sketch of the phase diagram of the four-dimensional Causal Dynamical Triangulations on the bare coupling constant  $K_0$ – $\Delta$  plane. We observe three phases: a *crumpled* phase, a *branched polymer* phase and the most interesting a genuinely four-dimensional phase. Right: Monte Carlo snapshot of a typical configuration in the genuinely four-dimensional phase. We plot the spatial volume distribution  $v_t$ .

In the model of Causal Dynamical Triangulations we have a distinction between time links and spatial links, allowing us to assign them different lengths. Such an asymmetry, not possible in the Euclidean version of Dynamical Triangulations, introduces the asymmetry parameter  $\Delta$  ( $\Delta = 0$  in the symmetric case). For large values of  $\Delta$  we observe the third, most interesting, phase. In this range of bare coupling constants, a typical configuration has a “bloblike” shape and behaves as a well defined four-dimensional manifold (see Fig. 1 right-hand side). The measurements of the Hausdorff dimensions confirm that at large scales the universe is genuinely four-dimensional [1]. All results presented in this paper were obtained for a total volume  $V_4 = 160\,000$  simplices, and for  $K_0 = 2.2$ ,  $\Delta = 0.6$ ,  $K_4^{\text{crit}} = 0.9$ . This point corresponds to the third phase.

## 5. Background geometry

The causality condition imposes on configurations a global foliation in the proper time. Due to this property each spatial slice has a well defined integer time coordinate  $t$  and a spatial three-volume  $v_t$ . The index  $t$  ranges from 1 to  $T$ , and because of time-periodic boundary conditions time slice  $t = T + 1$  is cyclically identified with time slice  $t = 1$ . The measurements of expectation values of observables are calculated performing averaging over Monte Carlo generated path integral samples, as described in (6). The Einstein–Hilbert action (2), as well as the Regge action (4), are invariant under the time translation  $t \rightarrow t + \delta$ . In order to perform a meaningful average of the spatial volume  $v_t$ , an appropriate time shift is needed, otherwise

the uniform distribution of volume would be obtained. The shift can be done by fixing a position of the “mass center” of the volume distribution  $v_t$  for each configuration included in the Monte Carlo average (6). The results obtained in simulations show that the average geometry (plotted in Fig. 2) is a de Sitter space,

$$\bar{v}_t \equiv \langle v_t \rangle \propto \cos^3(t/B), \quad (7)$$

where  $B$  is the time extension of the “blob”. This corresponds to the maximally symmetric solution of the classical Einstein equations with a positive cosmological constant,

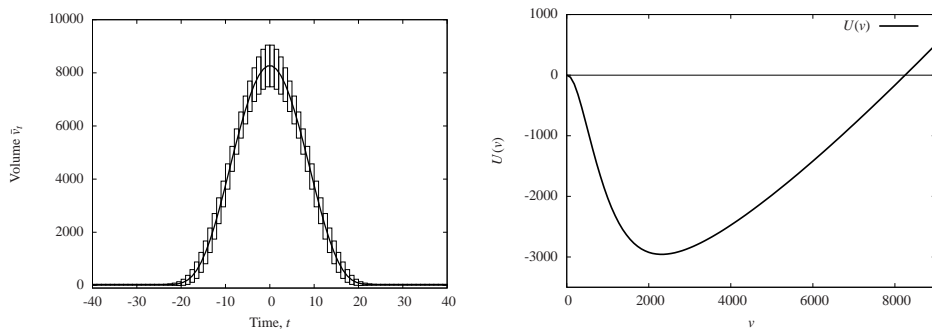


Fig. 2. Left: background geometry. Average spatial volume  $\bar{v}_t$  for  $K_0 = 2.2$ ,  $\Delta = 0.6$  and  $V_4 = 160\,000$ . The best fit  $A \cos^3(t/B)$  is indistinguishable from the numerical curve. The bars indicate the amplitude of quantum fluctuations. Right: the potential  $U(v)$  corresponding to the effective model with a small volume modification.

## 6. The minisuperspace model

The behavior of the spatial volume  $\bar{v}(t) \propto \cos^3(t/B)$  emerges as a classical solution of a minisuperspace model. This model assumes spatial homogeneity and isotropy, which means that all degrees of freedom except the volume are “frozen”. In the CDT model we have the opposite situation, no degrees of freedom are excluded, instead we integrate out all of them but the scale factor. Nevertheless, in both cases results demonstrate high similarity.

Let us introduce a spatially homogeneous and isotropic metric on a space-time with  $S^3 \times S^1$  topology,

$$ds^2 = dt^2 + v^{2/3}(t)d\Omega_3^2,$$

where  $v(t)$  is the volume of the spatial slice with a topology  $S^3$ . In this particular case, the Einstein–Hilbert action takes the form

$$S = \frac{1}{G} \int dt \int d\Omega \sqrt{g}(R - 6\lambda) = \frac{1}{G} \int \frac{\dot{v}^2}{v} + v^{1/3} - \lambda v dt. \quad (8)$$

and is called the minisuperspace action.

Restricting our considerations to the spatial volume  $v(t)$  we reduce the problem to one-dimensional quantum mechanics. The minisuperspace action (8) describes a motion of a particle in the well potential  $U(v) = -v^{\frac{1}{3}} + \lambda v$  plotted in Fig. 2. For small volumes finite size corrections are needed to regularize the potential near zero, so that it has a quadratic behavior. In this case, the universe remains for a long time at a zero volume, then suddenly makes an instant “bounce” and collapses back, giving the blob shape of  $\bar{v}(t)$ . The transition amplitudes of a quantum system can be calculated just as in the instanton problem.

### 7. Quantum fluctuations

The classical trajectory, *i.e.* the average spatial volume  $\bar{v}(t) \propto \cos^3(t)$ , is perfectly recovered in the minisuperspace model. This encourages us to state a question if quantum fluctuations around the background geometry are also correctly described by the action (8).

Let us denote the deviation of the spatial volume  $v(t)$  from the average  $\bar{v}(t)$  as  $x(t) = v(t) - \bar{v}(t)$ . In the semiclassical approximation, the spatial volume fluctuations  $x(t)$  are described by a Hermitian Sturm–Liouville operator  $P(t)$ , obtained in the quadratic expansion of the action

$$S[v = \bar{v} + x] \approx S[\bar{v}] + \frac{1}{2} \int x(t)P(t)x(t)dt. \tag{9}$$

For the minisuperspace action (8) expansion around the classical solution (7) gives

$$P(t) = -\partial_t \frac{1}{\bar{v}(t)} \partial_t - \left. \frac{\partial^2 U}{\partial v^2} \right|_{v=\bar{v}},$$

where  $U(v) = -v^{\frac{1}{3}} + \lambda v$ . Results obtained in the CDT framework are realized for a discrete time coordinate. In this case, a discretized, dimensionless version of the action (8) is

$$S[v] = \sum_{t=1}^T \left( \frac{c_1}{v_t} (v_{t+1} - v_t)^2 + c_2 (v_t^{1/3} + \lambda v_t) \right) \tag{10}$$

and the expansion (9) is

$$S[\bar{v} + x] \approx S[\bar{v}] + \frac{1}{2} \sum_{t,t'} x_t P_{tt'} x_{t'}.$$

The Sturm–Liouville operator  $P(t)$  is a matrix  $P_{tt'}$  with elements given by

$$\sum_{tt'} x_t P_{tt'} x_{t'} = \sum_t \underbrace{\frac{c_1}{\bar{v}_t}}_{k_t} (x_{t+1} - x_t)^2 - \underbrace{\left. \frac{\partial^2 U}{\partial v^2} \right|_{v=\bar{v}_t}}_{u_t} x_t^2. \tag{11}$$

The coefficients  $k_t$  correspond to the kinetic term, and  $u_t$  to the potential part.

Using Monte Carlo techniques we are able to measure not only the average volume  $\bar{v}_t$  at a time step  $t$ , but also the correlation matrix  $C$  of volume fluctuations

$$C_{tt'} \equiv \langle x_t x_{t'} \rangle,$$

also called the propagator. The brackets  $\langle \dots \rangle$  mean averaging over the whole ensemble of geometries, and can be approximated by a sum over statistically independent Monte Carlo configurations as in (6). There exists a direct relation between the propagator  $C$  and the matrix  $P$

$$C_{tt'} = \frac{1}{Z} \int x_t x_{t'} e^{-\frac{1}{2} \sum_{t,t'} x_t P_{tt'} x_{t'}} \prod_s dx_s = P_{tt'}^{-1}.$$

The propagator  $C$  can be measured using Monte Carlo techniques, in the same way as  $\bar{v}_t$  was measured. For the numerical convenience, we have fixed the total four-volume  $V_4 \equiv \sum_{t=1}^T v_t$  for every measurement. This constraint imposes on the covariance matrix  $C$  existence of a zero mode, namely the constant vector  $e^0$ ,

$$\sum_j C_{ij} e_j^0 = 0, \quad e_j^0 = \frac{1}{\sqrt{T}}.$$

The matrix  $P$  is, therefore, given as the inverse of  $C$  on the subspace orthogonal to the zero mode  $e^0$ ,

$$P = (C + A)^{-1} - A, \quad A_{ij} = e_i^0 e_j^0 = \frac{1}{T}.$$

Having calculated the covariance matrix  $C$ , we get the empirical Sturm–Liouville operator  $P$  which can be compared with the predictions of the minisuperspace model. Indeed the empirical  $P$  matrix has to a very good approximation a tri-diagonal structure being a sum of the potential and kinetic terms, as we expect from (11)

$$P = P^{\text{kin}} + P^{\text{pot}}.$$

The kinetic part  $P^{\text{kin}}$  is a tridiagonal symmetric matrix, such that the sum of the elements in a row or a column is always zero, and can be decomposed into parts linearly dependent on  $k_t$

$$P^{\text{kin}} = \sum_{t=1}^T k_t X^{(t)},$$

where  $X^{(t)}$  is a matrix corresponding to the discretization of the second time derivative  $\partial_t^2$  at a time  $t$ ,

$$X_{jk}^{(t)} = \delta_{tj}\delta_{tk} + \delta_{(t+1)j}\delta_{(t+1)k} - \delta_{(t+1)j}\delta_{tk} - \delta_{tj}\delta_{(t+1)k}.$$

Because we have to cut out the zero mode, the potential part  $P^{\text{pot}}$  is a projection of a diagonal matrix  $\text{Diag}(\{u_t\})$  on the subspace orthogonal to  $e^0$ ,

$$P^{\text{pot}} = (\mathbf{1} - A)\text{Diag}(\{u_t\})(\mathbf{1} - A) = \sum_{i=t}^T u_i Y^{(i)}, \tag{12}$$

where

$$Y_{jk}^{(t)} = \delta_{tj}\delta_{tk} - \frac{1}{T}(\delta_{tj} + \delta_{tk}) + \frac{1}{T^2},$$

and  $\mathbf{1}$  denotes the  $T \times T$  unit matrix. The kinetic part remains unaffected by the projection, since  $AP^{\text{kin}} = 0$ .

The decomposition of  $P$  into a “kinetic” and “potential” term, is done using the least square method. We find such values of  $\{k_t\}$  and  $\{u_t\}$ , that the matrix  $P^{\text{kin}} + P^{\text{pot}}$  is as close as possible to the empirical matrix  $P$ , *i.e.* we minimize the error function

$$\text{Tr} \left[ P - (P^{\text{kin}} + P^{\text{pot}}) \right]^2.$$

### 7.1. Kinetic term

If the predictions of the minisuperspace model are correct and the quantum fluctuations arise from the action (8), we expect, according to (11), a following behavior of the kinetic term,

$$k_t = \frac{c_1}{\bar{v}_t}. \tag{13}$$

We can use the fitted coefficients  $k_t$  and compare  $c_1/k_t$  with the directly measured average spatial volume  $\bar{v}_t$ . The comparison of  $c_1/k_t$  and  $\bar{v}_t$  is illustrated in Fig. 3 for a variety of four-volumes  $V_4$ . It is seen that the relation (13) is very accurate and, most important, the coupling constant  $c_1$ , which was determined independly for each four-volume  $V_4$ , really is independent of  $V_4$ .

The gravitational coupling constants  $G$  used in the continuum action (8) and the effective coupling constants  $c_1$  used in the discrete action (10) are related as derived in [7, 8],

$$G = c \frac{a^2}{c_1},$$

where  $c$  is a geometrical constant. Knowing  $G = \ell_{\text{Pl}}^2$  and  $c_1$  we can express the cut-off size  $a$  in terms of Planck length  $\ell_{\text{Pl}}$ . From the simulations for  $K_0 = 2.2$  and  $\Delta = 0.6$  we obtained  $a \approx 2\ell_{\text{Pl}}$  and the linear size of the universe build from 160 000 simplices is about  $20\ell_{\text{Pl}}$ .

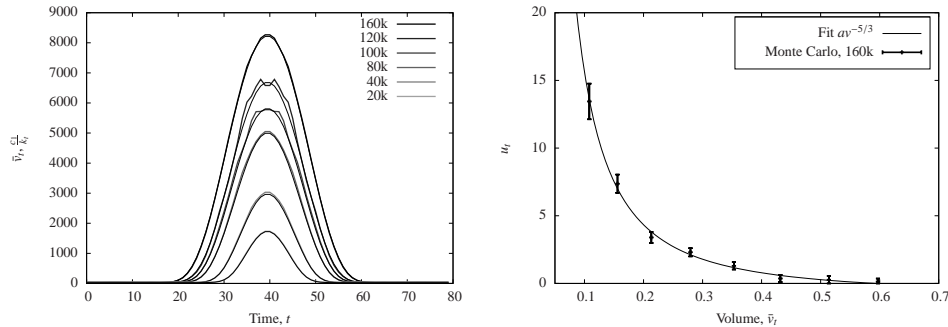


Fig. 3. Left: kinetic term: the directly measured expectation values  $\bar{v}_t$  (thin line), compared to  $c_1/k_t$  (thick line) extracted from the measured covariance matrix  $C$  for  $K_0 = 2.2$ ,  $\Delta = 0.6$  and various total volumes  $V_4$  ranging from 20 000 to 160 000 simplices. Right: potential term: the extracted second derivative of the potential  $u_t = c_2 U''(v_t)$  as a function of average spatial volume  $\bar{v}_t$ . The fit  $c_2 \bar{v}_t^{-5/3}$  presents the behavior expected for the minisuperspace model.

### 7.2. Potential term

Similarly, from (11) we expect the potential term  $u_t$  to behave like

$$u_t = c_2 U''(\bar{v}_t) = c_2 \bar{v}_t^{-5/3}, \quad U(v) = -v^{1/3} + \lambda v. \quad (14)$$

The extraction of  $u_t$  from  $P^{\text{pot}}$  is not an easy task, because it has large statistical errors. The main reason is that, due to the projection onto the space orthogonal to the zero mode, the interesting region of large volumes, and therefore small  $u_t$ , is affected by the huge contribution from the stalk, where the discretization effects are important. Secondly, the potential term is always sub-dominant to the kinetic term for individual spacetime histories in the path integral.

Fig. 3 shows the measured coefficients  $u_t$  extracted from the matrix  $P^{\text{pot}}$  as a function of average three-volume  $\bar{v}_t$  together with a fit  $c_2 \bar{v}_t^{-5/3}$ , corresponding to a potential  $c_2 v^{1/3}$ . In order to avoid the influence of the discretization effects, Fig. 3 includes data for volumes respectively larger than the kinematically allowed minimum, *i.e.* five tetrahedrons. It is seen that the relation (14) agrees very well with numerical data. Moreover, the coefficient  $c_2$  in front of Eq. (14) seems to be independent on  $V_4$ .

In summary, we conclude that the data allow us to reconstruct the action (8) with a good precision.

## 8. Conclusions

The Causal Dynamical Triangulations model of quantum gravity is very simple. It introduces a lattice regularization and Wick rotation, to calculate the path integral over the class of causal geometries with a global time foliation. We use Monte Carlo simulations to perform nonperturbative computation of the path integral.

We observe that a typical geometry, appearing in the path integral, represents a four-dimensional universe with well defined time and space extension. As a background geometry we obtained a de Sitter space, which exactly corresponds to the maximally symmetric solution of the classical Einstein equations in the presence of a positive cosmological constant. Quantum fluctuations of the spatial volume around the average geometry are also perfectly described by the minisuperspace model. Fluctuations of the three-volume are considerable, as can be seen in Fig. (2), and allow us to study quantum effects. Nevertheless they completely agree with the semiclassical description.

The gravitational constant  $G$  is responsible for a fluctuation amplitude and can be related to the measured effective coupling constant  $c_1$ . This allowed us to determine the cut-off size  $a$  and to estimate that the universe built of 160 000 simplices, a typical configuration size used in Monte Carlo simulations, has a radius of about 20 Planck lengths.

The author would like to thank Jerzy Jurkiewicz, Jan Ambjørn and Renate Loll for introducing him into this fascinating topic and for a fruitful collaboration. The author acknowledges support by ENRAGE (European Network on Random Geometry), a Marie Curie Research Training Network, contract MRTN-CT-2004-005616 and by COCOS (Correlations in Complex System), a Marie Curie Transfer of Knowledge Project, contract MTKD-CT-2004-517186.

## REFERENCES

- [1] J. Ambjørn, J. Jurkiewicz, R. Loll, *Phys. Rev.* **D72**, 064014 (2005).
- [2] J. Ambjørn, J. Jurkiewicz, R. Loll, *Nucl. Phys.* **B610**, 347 (2001).
- [3] J. Ambjørn, S. Varsted, *Nucl. Phys.* **B373**, 557 (1992).
- [4] C. Teitelboim, *Phys. Rev. Lett.* **50**, 705 (1983).
- [5] C. Teitelboim, *Phys. Rev.* **D28**, 297 (1983).
- [6] R.M. Williams, *Nucl. Phys. Proc. Suppl.* **B57**, 73 (1997) [[gr-qc/9702006](#)].
- [7] J. Ambjørn, A. Görlich, J. Jurkiewicz, R. Loll, *Phys. Rev. Lett.* **100**, 091304 (2008) [[hep-th/0712.2485](#)].
- [8] J. Ambjørn, A. Görlich, J. Jurkiewicz, R. Loll, *Phys. Rev.* **D78**, 063544 (2008).